Available online at www.sciencedirect.com
SCIENCE DIRECT®
Catalysis Today 98 (2004) 565–574
CATALYSIS TODAY
www.elsevier.com/locate/cattod

Towards an efficient process for small-scale, decentralized conversion of methane to synthesis gas: combined reactor engineering and catalyst synthesis

Dirk Neumann[a], Mark Kirchhoff[b], Götz Veser[a,b,*]

[a]*Department of Chemical Engineering, University of Pittsburgh, Pittsburgh, PA 15261, USA*
[b]*Max-Planck-Institut für Kohlenforschung, 45470 Mülheim an der Ruhr, Germany*

Available online 8 October 2004

Abstract

Anthropogenic methane emissions not only pose an increasing global problem but can also be seen as an untapped renewable resource for hydrogen or liquid fuel production. Utilization of this resource requires the development of efficient processes for small-scale, decentralized methane conversion. We see catalytic partial oxidation of methane to synthesis gas as an ideal candidate for such a process. In the present study, we investigate the effect of heat-integration, flow rate and catalyst stability on syngas yields over alumina-supported Pt and Rh catalysts in a reverse-flow reactor configuration. We furthermore demonstrate that novel high-temperature stable nanocomposite catalysts can dramatically lower the noble metal requirement for this reaction, improve catalyst stability and further increase synthesis gas yields. Finally, we demonstrate that the combination of the reverse-flow reactor with these nanocomposite catalysts exploits the efficiency of this reaction route very effectively while maintaining a simple and compact reactor design.

Keywords: Catalyst synthesis; Nanocomposite catalysts; Reverse-flow reactor

1. Introduction

Atmospheric methane concentrations have more than doubled since pre-industrial time, with currently about 70% of the worldwide methane emissions being of anthropogenic origin [1]. This raises concerns about the impact on the global climate, since methane is one of the most important so-called ''greenhouse gases'' with a global warming potential (GWP over the next 100 years) of about 23 (see Table 1) and an estimated climate forcing which is second only to CO_2 [1,2]. This estimated strong impact of methane on global climate changes in combination with the relatively short atmospheric lifetime of methane of about 8.4 years make methane a very attractive candidate for rapid impact measures to reduce anthropogenic climate changes.

Worldwide, wetlands (in particular rice paddies), ruminants, as well as landfills and other anaerobic waste management are the most significant anthropogenic contributors. The largest domestic US methane sources are landfills (34%) followed by domesticated livestock and emissions from the gas and oil industry (20% each) [3]. While net methane emissions from domestic landfills have shown a mild decline from about 10,000 Gg CH_4 in 1990 to about 9800 Gg in 2000, this decline has largely been due to flaring of methane emissions from landfills. Obviously, rather than solving the problem of methane emissions, this simply shifts the problem to the typical emissions from combustion processes (CO_2, NO_x, etc.).

However, methane emissions from anthropogenic sources, in particular from landfills and waste management, could be turned into a valuable renewable resource. The use of these resources depends vitally on the development of cheap and efficient technology to utilize its potential. While combustion of methane is a sufficiently simple and widely

* Corresponding author. Fax: +1 412 6249639.
E-mail address: gveser@pitt.edu (G. Veser).

0920-5861/$ – see front matter © 2004 Elsevier B.V. All rights reserved.
doi:10.1016/j.cattod.2004.09.010

Table 1
Main anthropogenic greenhouse gases along with their atmospheric concentrations, global warming potentials (GWP over 100 years), atmospheric lifetime, climate forcing and main anthropogenic sources (compiled from [1,2])

Gas	Formula (ppbv)	Pre-industrial concentration (ppbv)	1994 concentration	GWP	Atmospheric lifetime (years)	Climate forcing (W/m^2)	Main anthropogenic source
Carbon dioxide	CO_2	278000	358000	1	5–200	1.4	Combustion, cement production
Methane	CH_4	700	1721	23	8.4	0.7	Wetlands, ruminants, landfills
Nitrous oxide	N_2O	275	311	296	120	0.15	Fertilizers, combustion
Perfluoro-methane	CF_4	0	0.5	5700	50000	0.01	Aluminum production
CFC-12	CCl_2F_2	0	0.07	6200	102	0.35	Liquid coolants, foaming agent
Sulfur hexafluoride	SF_6	0	0.03	22000	3200	0.01	Dielectric fluid

available technology, the associated emissions of CO_2 and nitrous oxides typically pose new problems, particularly for small-scale applications where low NO_x burners would be too expensive and measures for CO_2 mitigation impractical. It would be much preferable if efficient technologies could be developed to convert methane to hydrogen for fuel cell-based power generation, or to synthesis gas (a mixture of CO and H_2), which could then further be converted to ultra-clean liquid fuels (the latter case being preferential due to the fact that it would also take care of the carbon management). In either case, methane conversion is only the first step, which needs to be followed by further clean-up or conversion steps, but in both cases this first step currently represents the largest portion of the investment cost and presently available technology has been developed and optimized for large-scale industrial processes rather than the small-scale processes needed to convert relatively small methane streams at distributed sources (such as municipal landfills).

In the following, we will give a very brief overview over current process alternatives for methane conversion to synthesis gas, and then report on recent steps in our research group towards an efficient small-scale process for methane utilization.

2. Synthesis gas from methane

At present, the main industrial route for the production of synthesis gas from methane is via steam reforming of methane (SRM) [4–6]. In this process methane is converted with water over Ni-based catalysts in a strongly endothermic reaction to yield CO and H_2 in a molar ratio of 1:3:

$$CH_4 + H_2O \rightarrow CO + 3H_2, \quad \Delta H_R = +206\,kJ/mol$$

The process is highly endothermic and is hence conducted in large, externally fired tubular reformers, which make SRM a major energy consumer in the chemical industry and result in significant emissions of combustion gases. A main problem of SRM is that only about half of the heat generated on the combustion side of the tubes is transferred to the reaction. At a large industrial site, the remaining waste heat can be integrated in the energy network, thus minimizing overall energy losses. This is not a possibility for decentralized processes and limits the efficiency of SRM for such applications.

This problem can be avoided if the combustion is directly coupled with the steam reforming reaction inside the tubular reformer, which is the basis of autothermal reforming of methane (ATR) [5,6]. In this process, oxygen is added to the CH_4/H_2O reactor feed to couple the endothermic steam reforming with the highly exothermic combustion of methane

$$CH_4 + 2O_2 \rightarrow CO_2 + 2H_2O, \quad \Delta H_R = -802\,kJ/mol$$

(Contrary to the often stated claim, ATR is in fact not a coupling of SRM with partial oxidation, but rather with total oxidation of methane as evident from a heat balance for the respective systems.) This results in a significantly simpler, energetically quite efficient process and requires a complete redesign of the reactor in which a burner is placed in front of a homogeneous reaction zone followed by a single catalyst bed. However, ATM technology is rather expensive and does not lend itself easily to adaptation for small-scale processes.

Partial oxidation of methane (POM) is the third alternative for synthesis gas production. In contrast to the previous reaction routes, this reaction is mildly exothermic, which opens the possibility for an autothermal process without the support of an additional combustion reaction

$$CH_4 + \frac{1}{2}O_2 \rightarrow CO + 2H_2, \quad \Delta H_R = -37\,kJ/mol$$

The reaction can be conducted non-catalytically, i.e. as a pure gas-phase reaction between methane and oxygen, or with the use of a catalyst. The homogeneous process has been commercialized by Shell and Texaco. While the lack of a catalyst is in principle an attractive feature, the process can only be conducted with pure oxygen to avoid NO_x formation, which makes it unpractical and uneconomical for small-scale applications.

Alternatively, partial oxidation can also be conducted catalytically (CPOM) at a wide range of conditions and with a number of different catalysts [7]. Particularly the noble metal catalyzed reaction route at high temperature and short contact time conditions has received much attention in recent years [8–11]. Like the non-catalytic POM process, the reaction is mildly exothermic, opening the possibility of autothermal processes. However, due to the presence of a

catalyst, the reaction can be conducted at much milder conditions than homogeneous POM with process temperatures of about 1000 °C. Moreover, the presence of a catalyst and the milder reaction conditions suppress homogeneous NO_x formation, making the use of air instead of oxygen possible. This greatly simplifies the process and drastically reduces overall cost. Due to the conceptual simplicity (single reaction pathway, no external heating), the reaction can be conducted in simple, single-pass tubular flow reactors. Finally, very high space–time yields can be achieved as a result of the extremely short contact times (<100 ms), allowing for highly compact CPOM reactors.

All these factors make CPOM an ideal candidate for small-scale, decentralized conversion of methane to synthesis gas. However, a thermodynamic analysis of the system indicates a significant problem with this simplified picture [12]: while the reaction is (mildly) exothermic, this exothermicity only yields an adiabatic temperature rise of about $\Delta T_{ad} \sim 250$ °C (for a stoichiometric methane/air feed), which is well short of the very high temperatures (>900 °C) which are thermodynamically required for optimal syngas yields. The temperatures in excess of 1000 °C which are experimentally observed in this reaction are therefore not due to the partial oxidation reaction itself, but rather due to combustion of some of the methane feed. The reaction yield is thus determined by a complex interplay between partial and total oxidation reactions: the combustion of methane results in high temperatures which shift the reaction equilibrium towards the partial oxidation route. At the same time, however, this formation of total oxidation products by definition also reduces syngas selectivities. Overall, this interplay thus limits attainable synthesis gas yields at autothermal operation.

While these limitations could be overcome via additional external firing of the process, this would annihilate some of the main advantages of the process, namely its simplicity and environmental friendliness. Another form of raising the reactor temperature is external pre-heating of the reactor feed as already shown by Hickman and Schmidt in their early studies [8]. This, however, relies on the availability of cheap (and clean) heat sources, which is typically not the case for decentralized processes.

This problem can be overcome by the use of heat-integrated reactors. In these multifunctional reactors the catalytic reaction is coupled with an internal heat-exchange between the hot product gases and the cold feed gases making efficient use of the mild exothermicity of the partial oxidation reaction itself [13,14]. We have previously shown that integrated, recuperative heat-exchange in a counter-current heat-exchange reactor (CCHXR) is a very simple way to raise the reactor temperatures and improve reaction yields [15,16]. However, as shown in the pioneering studies by Boreskov and Matros, regenerative heat-integration by flow reversal is a slightly more complex, yet much more efficient way of integrating heat in a catalytic reactor [17]. In this reactor concept, periodic switching of the flow-direction of the gases through the reactor results in a very efficient internal regenerative heat-exchange, which makes this concept particularly suitable for mildly exothermic reactions. In the following, we will present some recent results from our investigations of this reactor concept for the noble metal catalyzed catalytic partial oxidation of methane.

3. Heat-integrated reactor

3.1. Experimental set-up

The experimental set-up is explained in more detail in a previous report and will therefore only briefly be described here [12]. The reactor set-up is shown schematically in Fig. 1: a monolithic catalyst (18 mm diameter, 10 mm length) is positioned between two extruded inert monoliths (length: 110 mm) which act as heat reservoirs. Thus, cold reactants enter the catalyst bed where the reaction occurs. The heat of reaction raises the temperature of the catalyst, the product gases and thus the downstream inert zone. At reverse-flow operation, the gas flow through the reactor is then reversed at a certain time so that cold feed gases are now pre-heated by exchanging heat with this hot inert zone upon entering the reactor. The reactants thus hit the catalyst at already elevated temperatures, which are then again further raised by the heat of reaction. Upon exiting the catalyst zone, the hot product gases exchange heat with the ('new') downstream inert zone, cooling down the gases and heating up this inert zone. Upon the next flow reversal, this cooling-heating cycle is repeated again, this time in the opposite direction. If this flow reversal is repeated at an appropriate cycling frequency, a so-called ''periodic steady state'' is eventually reached, which is characterized by temperature and concentration profiles of two subsequent half-periods which are mirror images of each other. Overall, this results in very high reaction temperatures in the reaction zone and comparatively low temperatures at both reactor ends.

The necessary flow reversal is accomplished in the laboratory reactor via four magnetically operated valves which are synchronized in pairs. Catalyst temperatures are measured with thermocouples, and a double-oven gas chromatograph (Shimadsu) is used for a time-averaged, quantitative determination of species concentrations in the product gas stream. The experimental set-up (reactor operation and data acquisition) is fully computer-controlled (PC with NI DA/AD-boards and LabView software).

All results were obtained during reactor operation with air (rather than pure oxygen), since air will be the oxidant of choice for a decentralized process. For a direct comparison of the performance of a reverse-flow reactor with a conventional stationary reactor, the same reactor set-up is used for steady state experiments without switching of the flow direction. In this way, it is assured that all differences between steady state results and results at reverse-flow

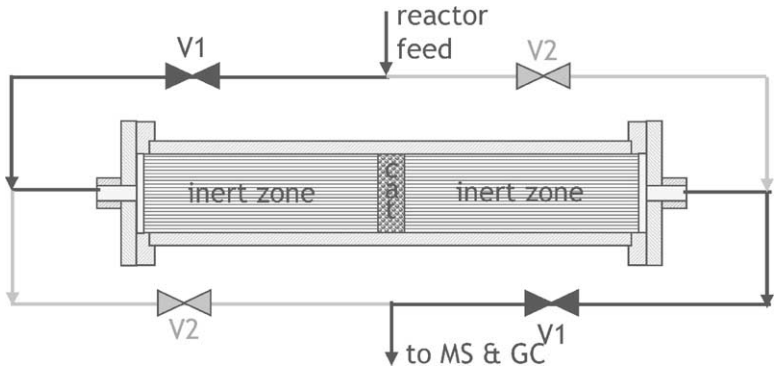

Fig. 1. Schematic drawing of the reactor set-up. The monolithic catalyst (cat) is positioned between two extruded monoliths which serve as inert zones. Four computer-controlled valves, which are operated in pairs (V1 and V2) allow for reversal of the flow direction in the reactor.

operation are due to differences in reactor operation rather than differences in the experimental set-up.

The catalysts used in these reactor studies are Pt- and Rh-coated alumina foam monoliths (45 ppi [pores per linear inch], Vesuvius High-Tech Ceramics). A closed noble metal film is deposited onto the alumina support via wet impregnation. For this purpose, the monoliths were coated with aqueous solutions of platinic chloride or rhodium(III) nitrate (Aldrich), dried for 1 h at 120 °C in air, calcined for 6 h at 600 °C in nitrogen, and then reduced in a highly diluted hydrogen stream (5% H_2 in N_2) for 6 h at 600 °C. This procedure was repeated as necessary to achieve weight loadings of 3–5 wt.% for all catalysts used.

3.2. Results with varying CH_4/O_2 ratio

Fig. 2 shows synthesis gas yields obtained over these catalyst in a conventional steady-state flow-tube reactor without flow-reversal (SS, left graph) and in a dynamically operated reverse-flow reactor (RFR, right graph) for a total reactor feed flow of 4 slm CH_4 in air (standard liter per minute, 1 slm = 1.67×10^{-5} m^3/s) with varying the CH_4/O_2 ratio in the reactor feed.

The results at steady state show that Rh is a significantly better catalyst for syngas production than Pt:CO yields over Rh are more than 10% and H_2 yields more than 20% above those for Pt. This agrees with previous studies by Hickman and Schmidt, who explained this difference in catalytic activities with the significantly higher activation barrier for OH formation on the Rh surface in comparison to Pt [8]. Furthermore, the results indicate that the stoichiometric point for the partial oxidation reaction (CH_4:O_2 = 2.0) has no particular significance for the reaction behavior. Instead, synthesis gas yields increase monotonously for both catalysts with decreasing CH_4/O_2 ratio. This is a strong indication that the reaction system is in both cases dominated by the availability of oxygen: as described above, some of the methane feed is combusted and supplies the heat necessary to achieve high autothermal temperatures. This severely limits the availability of oxygen for partial

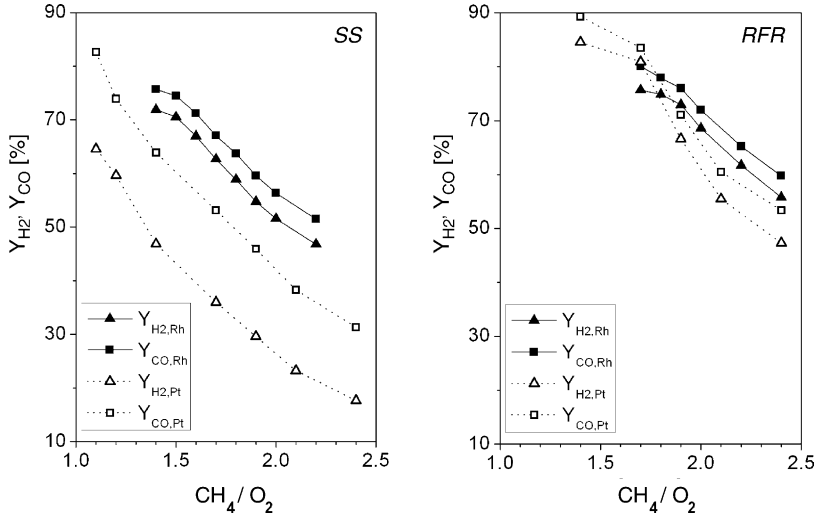

Fig. 2. Results from CPOM over a Pt (open symbols and dashed lines) and a Rh catalyst (full symbols and solid lines) at steady state reactor operation (SS, left graph) and reverse-flow operation (RFR, right graph). Synthesis gas yields are shown vs. CH_4/O_2 ratio. Experimental conditions were: V_{in} = 4 slm CH_4 in air, periodicity of flow reversal at RFR: 15 s.

oxidation since stoichiometrically four times as much oxygen per mol methane is consumed in total oxidation as in partial oxidation. Hence, methane conversion along the partial oxidation route is limited by the availability of oxygen, and any increase in oxygen supply – well beyond the stoichiometric point – results in higher syngas yields.

The right-hand graph shows the results with the same catalysts at reverse-flow operation. Flow direction was switched every 15 s to achieve regenerative heat-integration through the inert zones surrounding the catalysts. A very strong increase in syngas yields is apparent for both catalysts. While syngas selectivities over Rh increase by about 10% (absolute percentage points), syngas yields over Pt show a drastic improvement of about 15% for CO and almost 30% for hydrogen! Interestingly, the performance of the two catalysts approaches each other, with less than 5% difference for higher CH_4/O_2 ratios (>1.75) and Pt even surpassing Rh as catalyst at lower CH_4/O_2 (<1.75). Apparently, the poorer catalyst at steady state is rendered equal or even better through reverse-flow operation.

While homogeneous reactions could be suspected to play the 'equalizing' role at the increased reaction temperature at RFR, we have previously shown that homogeneous reactions do not contribute at all to CPOM at these short contact-time conditions [11]. Instead, the results can be understood as a direct result of heat-integration, as also reflected in the catalyst temperatures in Fig. 3. At steady state operation, the front end of either catalyst remains relatively cool with temperatures between 350 and 550 °C. Even though the strongly exothermic mix of partial and total oxidation in the catalyst zone leads to catalyst exit temperatures between 800 and 1150 °C, the cold feed gases which hit the catalyst at high flow velocity continuously cool the catalyst front edge. The reactants therefore first experience a rather cold catalyst zone, in which temperatures are in excess of ignition temperatures (which are around 400 °C), so that reaction can immediately occur, but which are much too low to yield good thermodynamic syngas yields. Therefore, this cold zone results in a significant amount of total oxidation which then drives catalyst temperatures up and allows for selective partial oxidation in the latter part of the catalyst [11].

At reverse-flow, this cold zone is completely avoided due to the efficient heat-integration, which pre-heats the feed gases to temperatures in excess of 800 °C at the catalyst entrance and leads to mean catalyst temperatures at either end of the catalyst which lie about 50–100 °C above the catalyst exit temperatures at SS. (Due to the nature of the reverse-flow operation, 'exit' and 'entrance' of the catalyst are not meaningful distinctions, since either end of the catalyst is exit in one half cycle and entrance in the following half cycle.) This heat-integration can also explain why the increase in synthesis gas yields is more pronounced for Pt than for Rh: since Pt is the less selective catalyst at steady state, product gases are significantly hotter when they leave the catalyst zone (see Fig. 3). Therefore, more sensible heat is available for heat-integration, and a stronger selectivity

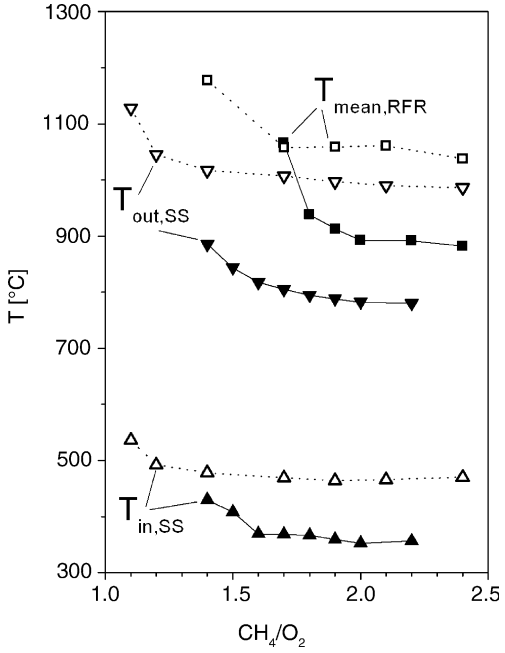

Fig. 3. Catalyst entrance (upward triangles) and exit temperatures (downward triangles) at steady-state reactor operation as well as mean catalyst end temperature at RFR operation (squares) during CPOM over a Pt (open symbols and dashed lines) and a Rh catalyst (full symbols and solid lines). Experimental conditions were: V_{in} = 4 slm CH_4 in air, periodicity of flow reversal at RFR: 15 s.

improvement results. Heat-integration can thus be a very efficient way to improve the performance of comparatively poor catalysts.

3.3. Results with varying flow rate

The above-described interplay between gas flow, reaction temperatures and synthesis gas yields is again apparent in the next set of experimental results: Fig. 4 shows synthesis gas yields over Pt and Rh catalysts with varying feed gas flow for a fixed CH_4/O_2 of 2.0 (O_2/N_2 = 1/4). The left graph again shows results at steady-state operation, while the right graph shows results at reverse-flow operation of the reactor.

Two effects can be seen from these results: at steady-state operation syngas yields go through a maximum around 3 slm feed gas flow with a strong decrease towards lower flow rates and a weak fall-off towards higher flow rates. In contrast to that, syngas yields at RFR continuously increase up to the maximum gas flow rate of 5 slm (higher flow rates were not possible with our experimental set-up).

The results can be explained in a straightforward way in view of the previous explanations: generally, low flow rates result in low heat production per unit time ($Q_R = V\Delta H_R$). However, since the very compact CPOM reactor shows significant heat losses to the environment at the high reaction temperatures, reduced heat production results in lower reactor temperatures and hence lower syngas yields. With increasing flow rate, heat production increases and hence temperatures and syngas yields increase. However, at the

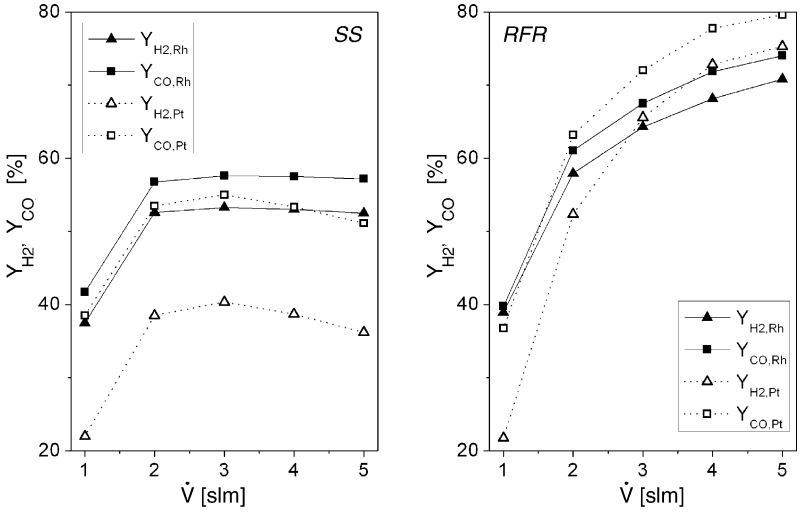

Fig. 4. Syngas yields vs. total volumetric inlet flow rate during CPOM over a Pt (open symbols and dashed lines) and a Rh catalyst (full symbols and solid lines) at steady state reactor operation (SS, left graph) and reverse-flow operation (RFR, right graph). Experimental conditions were: $CH_4/O_2/N_2 = 2/1/4$, periodicity of flow reversal at RFR: 15 s.

same time the cooling of the catalyst front edge by the cold feed gases is enhanced and ultimately starts to dominate over the effect of increasing heat production. This observation thus highlights the importance of the catalyst front edge in this reaction system. We had previously estimated from a detailed simulation study that most of the reaction is occurring in the first 2 mm of the catalyst, and that after 4–5 mm into the catalyst virtually no further reaction takes place any more [11]. This explains the observed strong sensitivity of the reaction system to changes in the catalyst entrance temperature.

At reverse-flow operation the cooling of the catalyst front edge with increasing flow rate is again suppressed due to the regenerative heat-integration. In fact, we have previously shown that at reverse-flow operation increasing flow rates lead to improved heat integration since it results in a more effective use of the heat reservoir that is represented by the inert zones [12]. Therefore, results at RFR operation show no improvement over SS results at the lowest flow rate where the inert zones are hardly utilized at all, and then show a continuously increasing trend with increasing flow rates.

It is tempting to speculate on the continuation of the curves for the syngas yields at RFR towards higher flow rates. It can be anticipated that this increase in syngas yields will continue towards higher flow rates until the heat capacity of the inert zones is exhausted, thermodynamic equilibrium is reached, or homogeneous reactions start to occur in the increasingly preheated inert zones. Since thermodynamics allows for 100% syngas yields at ambient pressure in this reaction system once autothermal limitations are broken, this is not a relevant limitation here. The other two limitations, however, could be overcome by appropriate reactor engineering measures: exhaustion of the heat capacity of the inert zones could be avoided by an increase in this heat capacity by replacing them with higher heat-capacity material, increasing their length, or using denser structures. The occurrence of homogeneous reaction at higher reaction temperatures is more difficult to suppress, but can be achieved by reducing the residence time of the gases in the inert zones. Thus, it seems that it should be possible to achieve further significant increases in the already very high CPOM reactor throughput through the use of regenerative heat-integration!

3.4. Catalyst stability

A significant problem at the extreme process temperatures of CPOM is catalyst stability. While all catalyst deactivate eventually in a catalytic process, the extreme conditions of CPOM accelerate the process significantly. It can be expected that this deactivation is further accelerated by the heat-integration due to the further increased reaction temperatures. The stability of the Pt and Rh catalysts at SS and RFR conditions was therefore further investigated.

Results are shown in Fig. 5, where the left graph shows syngas yields for the Pt catalyst at SS (open symbols and dashed lines) and RFR conditions (closed symbols and solid lines) versus time-on-stream, while the right graph shows the same results for the Rh catalyst.

It is immediately apparent that the Pt catalyst shows severe deactivation both at SS and RFR conditions, while Rh appears to be stable at both conditions. Apparently, reactor operation does not change the stability of the catalysts qualitatively. RFR operation thus does not seem to have the expected detrimental effect on catalyst stability. In fact, the Pt results even indicate a *reduced* deactivation at reverse-flow conditions: while hydrogen yields drop by 27% (from 47% to 20%) and CO yields by 20% (from 59% to 39%) over 20 h at steady-state conditions, the corresponding decreases

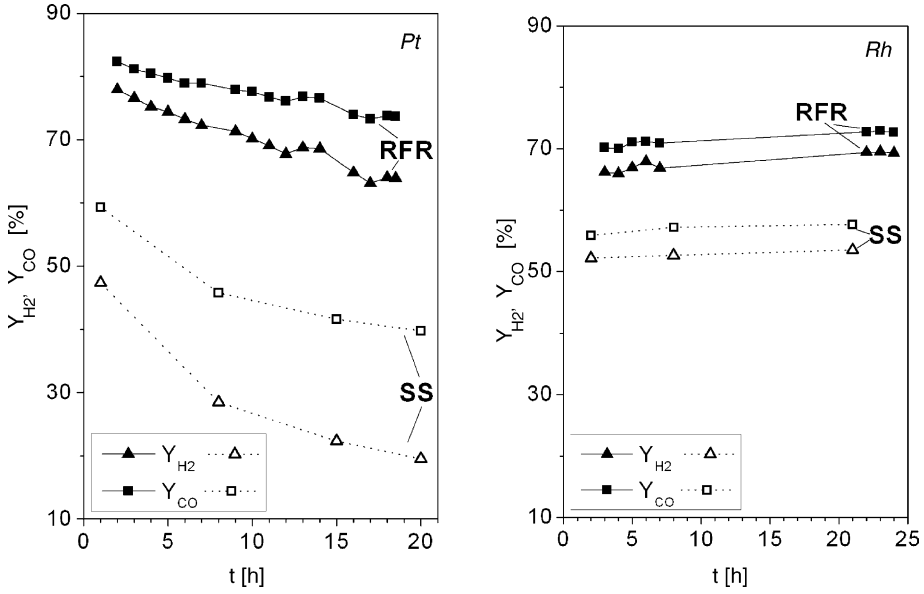

Fig. 5. Syngas yields vs. time-on-stream during CPOM over a Pt (left graph) and a Rh catalyst (right graph) at steady state reactor operation (SS, open symbols and dashed lines) and reverse-flow operation (closed symbols and solid lines). Experimental conditions were: $CH_4/O_2/N_2$ = 2/1/4, total inlet flow rate V_{in} = 3 slm, periodicity of flow reversal at RFR: 15 s.

are only 14% and 9%, respectively, at RFR, i.e. only about half as strong.

This surprising observation can once more be traced back to the heat-integration at reverse-flow reactor operation: the decreasing activity of the deactivating catalyst is thermally over-compensated by the decreasing selectivity of the reaction so that overall increasing reactor temperatures result. While at steady state these temperatures simply lead to increased exit gas temperatures, reverse-flow operation leads to a (partial) re-integration of this additional heat into the system. Therefore, regenerative heat-integration results in an intrinsic compensation of the effects of catalyst deactivation and thus an apparent reduction in the rate of catalyst deactivation.

While this effect is an unexpected benefit from heat-integration in this system, the rate of deactivation of the Pt catalyst nevertheless renders this catalyst impractical for technical application, in particular for decentralized processes where low cost and low maintenance is imperative for a successful implementation of a new technology.

4. Novel catalysts

In light of the above results, it seems that Rh should be the catalyst of choice for this reaction system. However, Pt has at least two significant advantages over Rh: it allows for a particularly easy start-up of the reactor, since H_2/O_2 mixtures ignite at room temperature over Pt catalysts [15]. This means that a mixture of air with some of the product gas (which would need to be temporarily stored during reactor shut-down) could serve as an easy start-up mixture for reactor operation. Since ease of reactor operation is a crucial factor for small-scale, decentralized processes, where highly trained personnel may not be available to operate the equipment, this easy start-up makes Pt very attractive for such processes. Furthermore, Rh is generally significantly cheaper than Pt. Although noble metal prices vary widely over time and are difficult to predict, the average price of rhodium over the past 5 years was about twice that of platinum (US$ 1160 versus US$ 610 per troy ounce). Since low cost is another key consideration, this strongly favors the use of Pt over Rh. We therefore investigated novel ways to achieve a more stable Pt-based catalyst for this reaction system.

4.1. Catalyst synthesis

The synthesis is based on a reverse-microemulsion templated sol–gel synthesis of nanometer-sized catalyst particles [18,19]. This synthesis route was applied both to Pt as the active component of the catalyst as well as to a high-temperature stabilized alumina support (barium hexaaluminate, BHA) which has been developed about 10 years ago by Arai and Machida for high-temperature combustion applications [20].

The steps in the catalyst synthesis are summarized in Fig. 6. An inverse (i.e. water-in-oil) microemulsion is formed by combining water, *iso*-octane and one of several different non-ionic surfactants (Neodol, Lutensol, and others). Then, an aqueous solution of hexachloro platinic acid was added to incorporate the catalytically active (noble) metal component. In a next step, a stoichiometric mixture of aluminum- and barium-alkoxides in *iso*-octane was slowly added to the

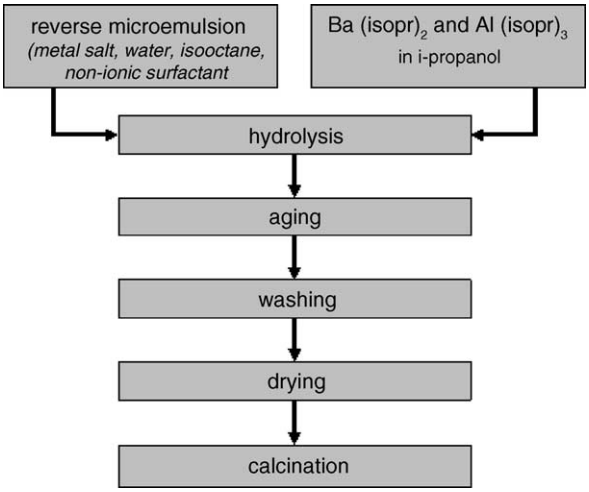

Fig. 6. Steps in the synthesis of the PtBHA nanocomposite catalyst.

microemulsion, where hydrolysis takes place. The microemulsion was aged for 48–72 h under constant stirring before the phases were separated by thermally induced phase separation (TIPS). The resulting gel was washed several times to remove the surfactant, and finally the material was vacuum dried and calcined at 600 °C.

The obtained powders were loosely agglomerated nanocomposites of very homogeneously distributed metal particles in a hexa-aluminate matrix [22] and were used as synthesized. Hundred milligrams of the powder were placed between two ceramic mats, sandwiched between two extruded cordierite monoliths and placed in the reactor as described above.

4.2. Catalyst tests

Results from the catalytic tests with these new catalysts are shown in Fig. 7: synthesis gas yields (left graph) and catalyst temperatures (right graph) are shown versus CH_4/O_2 ratio (with O_2/N_2 = 1/4) for a total inlet gas flow of 3 slm at steady-state reactor operation.

It can clearly be seen that this novel nanocomposite catalyst is far superior to the conventional Pt catalyst (compare to Fig. 2, left graph). Synthesis gas yields of up to 83% for hydrogen and up to 76% for CO are achieved for CH_4/O_2 = 1.2. This not only surpasses the results for the conventional Pt catalyst by about 10%, but even surpasses the results over the Rh catalyst at SS conditions. Interestingly, hydrogen yields are higher than CO yields for this novel catalysts, while CO yields were significantly higher than H_2 yields for both conventional catalysts at all conditions. This could be an indication that the reaction mechanism over the nanocomposite catalyst is in fact different from the mechanism over the conventional catalysts, but further investigations are needed to substantiate such a statement and elucidate possible differences in the reaction mechanisms.

The excellent results are all the more remarkable considering that the complete catalyst load in the reactor was only a 100 mg sample with about 8 wt.% Pt, i.e. the high syngas yields were achieved with only ∼8 mg Pt compared to more than 200 mg noble metal on the conventional catalysts! To test the limits of this unusually high catalyst activity, we varied the Pt content in the nanocomposite catalyst by varying the amount of Pt salt in the microemulsion. This resulted in unchanged sizes in the primary Pt nanoparticles, but a reduced number density of these particles in the nanocomposite material.

Fig. 8 shows the results of the catalytic tests with these materials: synthesis gas yields are shown for a total inlet gas stream of 3 slm and $CH_4/O_2/N_2$ = 2/1/4. One can see that synthesis gas yields increase with increasing Pt content of the catalyst and reach a plateau at 10 wt.% Pt. However, the initial increase of catalyst activity is particularly steep so that less than 4 wt.% Pt suffice already to achieve 90% of this final activity, and less than 1 wt.% Pt (corresponding to

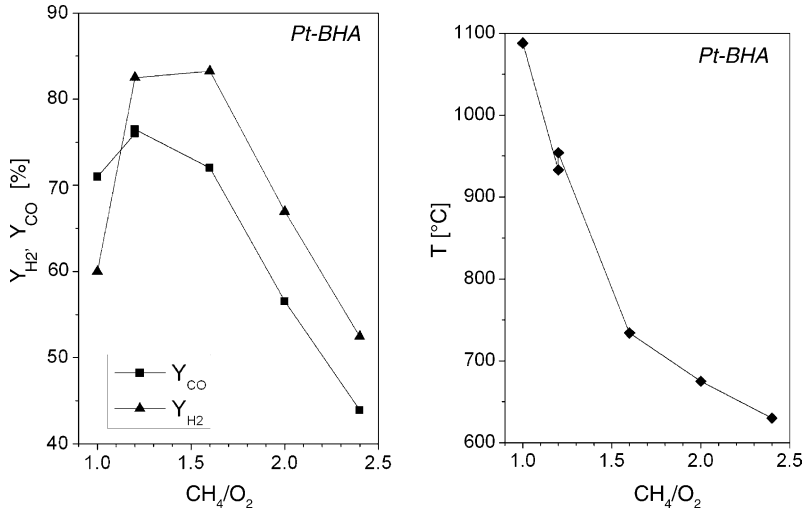

Fig. 7. Results from CPOM over a novel nanocomposite PtBHA catalyst at steady-state reactor operation. CO yields (left graph, squares) and hydrogen yields (left graph, triangles) as well as catalyst temperatures (right graph) are shown vs. CH_4/O_2 feed ratio with O_2/N_2 = 1/4 and total volumetric inlet flow V_{in} = 3 slm.

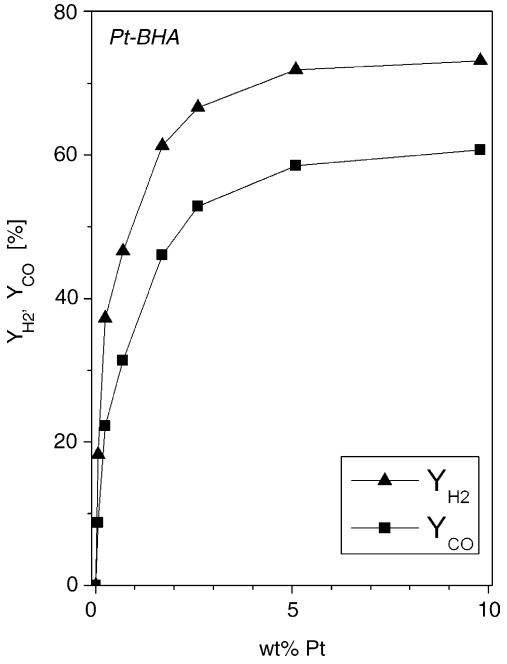

Fig. 8. Results from CPOM over a novel nanocomposite PtBHA catalyst at steady-state reactor operation. CO yields (squares) and hydrogen yields (triangles) are shown vs. Pt content of the catalyst. Experimental conditions were: $CH_4/O_2/N_2$ = 2/1/4, total volumetric inlet flow V_{in} = 3 slm.

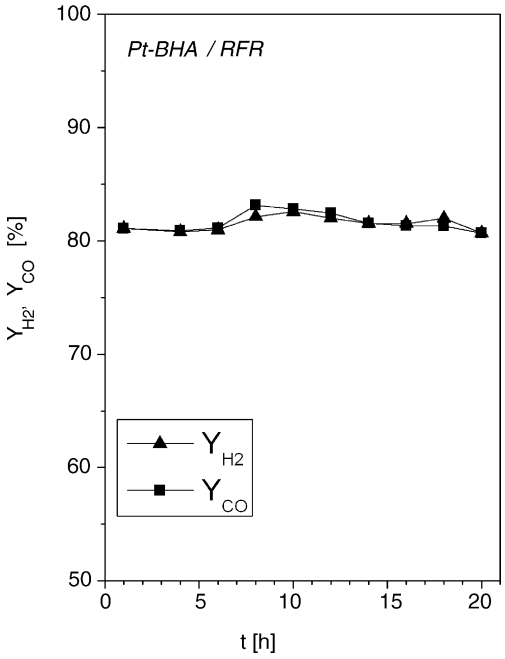

Fig. 9. Results from CPOM over a novel nanocomposite PtBHA catalyst at reverse-flow reactor operation. CO yields (squares) and hydrogen yields (triangles) are shown vs. time-on-stream. Experimental conditions: $CH_4/O_2/N_2$ = 2/1/4, total volumetric inlet flow V_{in} = 3 slm, periodicity of flow reversal = 15 s.

less than 1 mg Pt!) is needed to achieve results which are comparable to the SS results with the conventional Pt catalyst (Fig. 2). Clearly, these novel catalysts show an extremely high activity and selectivity for the conversion of methane to synthesis gas with a noble metal requirement which is about two orders of magnitude below that of the conventional catalysts.

As a final step, we tested the performance and stability of the nanocomposite catalysts at reverse-flow conditions as a first test on the improvements possible through the combination of the highly efficient integrated reactor concept with these novel catalysts. Results are shown in Fig. 9, where syngas yields are shown versus time-on-stream for a total gas flow of 3 slm and $CH_4/O_2/N_2$ = 2/1/4 over a 100 mg PtBHA sample with about 8 wt.% Pt and a periodicity of the flow reversal of 15 s.

One can see that again that syngas yields are strongly improved by the reverse-flow reactor operation. While steady-state operation at the same conditions gave CO yields of 57% and H_2 yields of 66% (see Fig. 7), both yields increase to about 81–82% at RFR. This improvement is not as dramatic as the improvements seen at RFR operation for the conventional Pt catalyst, the more selective reaction (and hence lower potential for heat-integration) explain this observation. Overall, these results lie well above the results achieved with any of the other catalysts at these reaction conditions. Further improvements should be possible by reducing the CH_4/O_2 ratio in the feed gas, and by adjusting the periodicity of the flow reversal, which we have previously shown to be a very important reactor operating parameter at RFR operation [21].

It seems noteworthy to point out that these results are the only results in our investigation where equal selectivities towards CO and H_2 are observed, and thus the ''ideal'' syngas ratio of $CO:H_2$ = 1:2 is achieved. This ratio is required for liquid fuel production from syngas via Fischer–Tropsch processes or methanol synthesis. The fact that this syngas ratio is in fact the stoichiometric product ratio of CPOM is often cited as one of the most significant advantages of CPOM over other syngas routes (since the product gas does not need any further adjustment of the syngas ratio in secondary reformer or water-gas-shift reactors). However, this ratio is rarely achieved in practice since any amount of total oxidation which occurs in parallel to the partial oxidation route will shift this ratio away from 2.0. The achievement of equal syngas yields is thus a strong indicator for the extremely high selectivity of this catalyst towards synthesis gas formation.

Most remarkably however, no catalyst deactivation is observed for the nanocomposite catalyst over the duration of the experiment. This is in stark contrast not only to the strong deactivation observed above for the conventional Pt catalyst, but also to the expectation that noble metal nanoparticles should show very rapid and severe sintering at these extreme reaction conditions. We had previously observed this unusual stability of these nanocomposite catalysts in a simple test-tube experiment over the duration of 100 h [20]. While the rather brief time-on-stream of only about 20 h in

the present experiment does not allow definite conclusions about the long-term stability of these catalysts over the time scales required in practical applications (typically at least > 1000 h), it confirms that these materials have the potential to be developed into highly efficient catalysts for high-temperature catalytic partial oxidation reactions.

5. Summary

In this report, we attempted to give a brief overview over some of the main technological routes for methane utilization via synthesis gas formation with an emphasis on efficient small-scale, decentralized processes for the capture and utilization of methane emissions from anthropogenic sources such as landfills and waste water treatments. Catalytic partial oxidation of methane at high-temperature, millisecond contact-time conditions was presented as a particularly well-suited reaction route for such processes due to the simplicity of the reaction and the compactness of the reactors.

We demonstrated that the efficiency of this reaction can be significantly improved via heat-integrated reactor concepts, in particular regenerative heat-integration by reverse-flow reactor operation. Strong improvements in synthesis gas yields over Pt and Rh catalysts were observed. The integrated reactor concept maintains the compactness of the reactor and keeps the process independent of external heat sources. An appropriately designed reverse-flow reactor should allow further increases in the reactor throughput over the already extremely high values achieved in the current laboratory reactor. Furthermore, this mode of reactor operation also leads to an effective containment of the very high reaction temperatures inside the catalyst zone, keeping both reactor ends as well as the product gas stream comparatively cool, which greatly facilitates handling of the reactor as well as of the product gas stream.

While the conventional Pt catalyst showed strong deactivation at the extreme conditions of CPOM, a novel nanocomposite catalyst not only added the necessary catalyst stability but also lead to further increases in syngas yields while dramatically lowering the noble metal requirement by as much as two orders of magnitude. These catalysts thus form a perfect complement to the heat-integrated reactor concept, lowering cost while further improving performance. The achieved syngas yields in excess of 80% at autothermal conditions compare quite favorably with existing industrial processes while being based on a very simple, compact process operated with air.

Overall, we see the combined development of the heat-integrated reactor concept as well as novel catalysts which withstand these extreme reaction conditions as a significant step towards an efficient and economical process for methane utilization in small-scale, remote and decentralized locations.

References

[1] Intergovernmental Panel on Climate Change (IPCC), Climate Change 2001: A Scientific Basis, Cambridge University Press, Cambridge, 2001.
[2] J.E. Hansen, M. Sato, Proc. Natl. Acad. Sci. 98 (2001) 14778–14783.
[3] EPA report ''Inventory of U.S. Greenhouse Gas Emissions and Sinks'', 2001.
[4] I. Dybkjaer, Fuel Process. Technol. 42 (1995) 85–107.
[5] K. Aasberg-Petersen, J.H. Bak Hansen, T.S. Christensen, I. Dybkjaer, P. Seier Christensen, C. Stub Nielsen, S.E.L. Winter Madsen, J.R. Rostrup-Nielsen, Appl. Catal. A 221 (2001) 379–387.
[6] J.R. Rostrup-Nielsen, Catal. Today 71 (2002) 243–247.
[7] A.P.E. York, T. Xiao, M.L.H. Green, Top. Catal. 22 (2003) 345–358.
[8] D. Hickman, L.D. Schmidt, Science 259 (1993) 343–346.
[9] L.D. Schmidt, M. Huff, S. Bharadwaj, Chem. Eng. Sci. 49 (1995) 3981–3994.
[10] L. Basini, K. Aasberg-Petersen, A. Guarinoni, M. Ostberg, Catal. Today 64 (2001) 9–20.
[11] G. Veser, J. Frauhammer, Chem. Eng. Sci. 55 (2000) 2271–2286.
[12] D. Neumann, G. Veser, AIChE J., in press.
[13] D. Agar, W. Ruppel, Chem. Ing. Technol. 60 (1988) 731–741.
[14] G. Kolios, J. Frauhammer, G. Eigenberger, Chem. Eng. Sci. 55 (2000) 5945–5967.
[15] U. Friedle, G. Veser, Chem. Eng. Sci. 54 (1999) 1325–1332.
[16] G. Veser, J. Frauhammer, U. Friedle, Catal. Today 61 (2000) 55–64.
[17] G.K. Boreskov, Y.S. Matros, Appl. Catal. 5 (1983) 337–343.
[18] M. Boutonnet, J. Kizling, P. Stenius, G. Maire, Coll. Surf. 5 (1982) 205.
[19] A.J. Zarur, J.Y. Ying, Nature 403 (2000) 65–67.
[20] H. Arai, M. Machida, Appl. Catal. A 138 (1996) 161–176;
J. Schicks, D. Neumann, U. Specht, G. Veser, Catal. Today 81 (2003) 287–296.
[21] D. Neumann, V. Gepert, G. Veser, Ind. Eng. Chem. Res., in press.
[22] M. Kirchhoff, U. Specht, G. Veser, in: G. Emig, et al. (Eds.), Innovation in the Manufacture and Use of Hydrogen, DGMK Publishing, Hamburg, 2003, pp. 33–40.